Examining the impact of heterogeneous nitryl chloride production on air quality across the United States

G. Sarwar[1], H. Simon[2], P. Bhave[1], G. Yarwood[3]

[1] National Exposure Research Laboratory, U.S. Environmental Protection Agency, Research Triangle Park, North Carolina, USA
[2] Office of Air Quality Planning and Standards, U.S. Environmental Protection Agency, Research Triangle Park, North Carolina, USA
[3] ENVIRON International Corporation, Novato, California, USA

Abstract

The heterogeneous hydrolysis of dinitrogen pentoxide (N_2O_5) has typically been modeled as only producing nitric acid. However, recent field studies have confirmed that the presence of particulate chloride can alter the reaction product to produce nitryl chloride ($ClNO_2$) which can undergo photolysis to generate chlorine atoms and nitrogen dioxide (NO_2). Both chlorine and NO_2 can affect atmospheric chemistry and air quality. We present an updated gas-phase chlorine mechanism that can be combined with the Carbon Bond 05 mechanism and incorporate the combined mechanism into the Community Multiscale Air Quality modeling system. We then update the current model treatment of heterogeneous hydrolysis of N_2O_5 to include $ClNO_2$ as a product. The model, in combination with a comprehensive inventory of chlorine compounds, reactive nitrogen, particulate matter, and organic compounds, is used to evaluate the impact of the heterogeneous $ClNO_2$ production on air quality across the United States for the months of February and September in 2006. The heterogeneous production can increase $ClNO_2$ in coastal as well as many in-land areas in the United States. Particulate chloride derived from sea-salts, anthropogenic sources, and forest fires can activate the heterogeneous production of $ClNO_2$. With current estimates of tropospheric emissions burden, it modestly enhances monthly mean 8-hr ozone (up to 1-2 ppbv or 3-4%) but can cause large increases (up to 13 ppbv) in isolated episodes. It can also substantially reduce the mean total nitrate by (up to 0.8-2.0 $\mu g/m^3$ or 11-21%). Modeled $ClNO_2$ accounts for up to 3-4% of the monthly mean total reactive nitrogen. Sensitivity results of the model suggest that $ClNO_2$ formation is limited more by the presence of particulate chloride than by the abundance of N_2O_5.

Keywords: chlorine, nitryl chloride, $ClNO_2$, heterogeneous reaction, ozone, nitrate, N_2O_5

1.0 Introduction

Recent studies suggest that chlorine chemistry can affect air quality in coastal and industrial areas of the United States (Chang et al., 2002; Knipping and Dabdub, 2003; Tanaka et al., 2003a; Chang and Allen, 2006; Sarwar and Bhave, 2007, Simon et al., 2009). These studies have evaluated the effects of naturally- and anthropogenically-derived chlorine on ozone (O_3). First, Knipping and Dabdub (2003) reported that chlorine released via heterogeneous reactions on sea-salt particles can increase daily maximum 1-hr O_3 by up to 4 parts-per-billion (ppbv) in the Los Angeles area of California. Chang et al. (2002) and Chang and Allen (2006) concluded that industrial chlorine emissions can increase O_3 by up to 10-16 ppbv in the Houston area of Texas. Finally, Sarwar and Bhave (2007) found that anthropogenic chlorine emissions can increase daily maximum 8-hr O_3 by up to 4 ppbv in New York/New Jersey and 8 ppbv in the Houston areas.

In the past few years a new chlorine-containing species, nitryl chloride ($ClNO_2$), has been implicated as a major pathway for the production of reactive chlorine. Photolysis of $ClNO_2$ generates chlorine atoms (Cl) and nitrogen dioxide (NO_2); each can alter atmospheric chemistry and air quality. Finlayson-Pitts et al. (1989) first suggested that $ClNO_2$ could be an intermediate between aqueous-phase chloride and gas-phase chlorine radicals, but measurement technology did not exist to confirm this hypothesis in the ambient atmosphere. In the 2006 TEXAQS II field study, Osthoff et al. (2008) measured atmospheric $ClNO_2$ for the first time. They report a peak value of greater than 1.0 ppbv near Houston. Results of several other recent field campaigns also suggested the presence of relatively high levels of $ClNO_2$ in coastal as well as in-land areas (Thornton et al., 2010, Mielke et al., 2010, Mielke et al., 2011). These studies suggest that the main formation pathway for $ClNO_2$ is heterogeneous hydrolysis of dinitrogen pentoxide (N_2O_5) in the presence of particulate chloride. Simon et al. (2009) investigated the impact of measured $ClNO_2$ concentrations on O_3 in Houston using the Comprehensive Air quality Model with extensions (CAMx) and reported that it can enhance O_3 by up to 1.5 ppbv. While the Simon et al. (2009) study suggests $ClNO_2$ can modestly affect O_3 in Houston, little is known about the importance of $ClNO_2$ in other areas and seasons. In the current study, we examine the impacts of the heterogeneous $ClNO_2$ production on air quality in the United States using state-of-the-science knowledge about chlorine chemistry and a detailed inventory of chlorine emissions.

2.0 Methodology

This study uses the Community Multiscale Air Quality (CMAQ) modeling system (version 5.0; beta version) (Binkowski and Roselle, 2003; Byun and Schere, 2006; Foley et al., 2010) to simulate air quality. Evaluations for the CMAQ modeling system against ambient measurements have shown that the CMAQ model has considerable skill is simulating O_3 and fine particles ($PM_{2.5}$) (Eder and Yu, 2006; Appel et al., 2007; Foley et al., 2010). The modeling domain covers the entire United States and consists of 299 x 459 horizontal grid-cells with a 12-km resolution (see Figure 1). The model contains 34 vertical layers with a surface layer height of 36-meters. Model simulations were performed for February and September in 2006. Monthly mean boundary conditions were used for the study. CMAQ results from a previous model simulation are used as initial conditions for this work. To further minimize the impact of initial conditions on predicted results, the model simulation started five days prior to the

actual simulation periods. Meteorological fields were obtained from the Weather Research and Forecasting (version 3.3) model (Skamarock et al., 2008).

2.1 Emissions

The 2005 National Emissions Inventory (http://www.epa.gov/ttn/chief/net/2005_nei_point.pdf) is used to generate model-ready emissions using the Sparse Matrix Operator Kernel Emission (SMOKE) (Houyoux et al., 2000). The Biogenic Emissions Inventory System (version 3.14) is used to compute biogenic emissions from soil and vegetation (Schwede et al., 2005). Emissions of molecular chlorine (Cl_2) and hydrochloric acid (HCl) are included in the 2005 National Emissions Inventory. In addition, the fine-particulate emissions are speciated into the standard suite of compounds and trace elements (Reff et al., 2009). The largest sources of anthropogenic particulate chloride include paved and unpaved road dust, agricultural soil, wildfires, agricultural burning, coal/wood combustion, and diesel exhaust (Reff et al., 2009). Coarse particulate matter is also speciated to include particulate chloride. Road salt, one potentially important source of particulate chloride, is missing in the inventory. Fine and coarse sea-salt emissions (both open-ocean and surf-zone) are calculated in-line in CMAQ (Kelly et al., 2010).

2.2 Gas-phase chlorine chemistry

This study expands the CB05TU chemical mechanism (Whitten et al., 2010) to include additional chlorine chemistry. CB05TU builds on earlier work by Gery et al. (1989) and Yarwood et al. (2005) and includes 172 reactions involving 60 chemical species. These chemical mechanisms have been previously evaluated in the CMAQ model (Sarwar et al., 2008; Sarwar et al., 2011). Tanaka et al. (2003b) developed a chlorine mechanism consisting of 13 chemical reactions for use with an earlier version of this chemical mechanism. Here, we modify, and extend the chlorine mechanism of Tanaka et al. (2003b) for use with the CB05TU mechanism. Atmospheric reactions in the updated chlorine mechanism are shown in Table 1. Rate constants for these reactions were updated using the recommendations from the International Union of Pure and Applied Chemistry (IUPAC) (Atkinson et al., 2005).

The new chlorine mechanism updates the chemistry developed by Tanaka et al. (2003b) in several ways. First, the chemistry is adjusted to new chemical species in the CB05TU mechanism. For example, the earlier mechanism grouped all aldehydes into a single lumped species, but the CB05TU mechanism splits acetaldehyde out from higher aldehydes. Similarly, the older mechanism included one olefin species, while the current mechanism separates compounds with internal carbon-carbon double bonds from those with a terminal carbon-carbon double bond (alk-1-enes). The new chlorine chemistry has been adjusted to account for these and other new species definitions. The reactions of formaldehye, acetaldehyde, and higher aldehydes with Cl are similar to their reactions with OH. The only exception is that the reaction with Cl produces HCl compared to H_2O produced from reactions with OH. The products of the reaction between higher aldehydes and Cl are uncertain because there may be hydrogen atom abstraction at the paraffinic carbon atoms of higher aldehydes.

Reaction products for terminal olefins with chlorine assume that reaction with the carbon-carbon double bond proceeds by addition, leading to cleavage of the double bond producing an acyl chloride (represented by formyl

chloride) and an aldehyhyde (represented as 33% acetaldehyde and 67% higher aldehydes). The rate constant for the reaction between Cl and terminal olefins (R14) is an average over the absolute rate constants for the alkenes presented in Tanaka et al. (2003b). The rate constant for the reaction of chlorine with internal olefins (R15) is estimated as the rate constant for Cl reacting with a terminal olefin bond and two paraffin bonds. The products assume that reaction proceeds 70% by Cl addition to the C=C bond and 30% by hydrogen atom abstraction from attached alkyl groups. Cl addition leads to cleavage of the double bond producing an acyl chloride (represented by formyl chloride) and an aldehyhyde (represented as 65% acetaldehyde and 35% higher aldehydes). The products for hydrogen atom abstraction pathway are assumed to be HCl, higher aldehydes, and terminal olefins.

Second, the new chlorine chemistry includes more reactions of chlorine radicals with organic species including methanol, ethanol, aromatics, aldehydes, and ethane. The reaction between ethane and OH proceeds via the abstraction pathway and produces (in the presence of oxygen) ethyl peroxy radical and H_2O. The reaction of ethyl peroxy radical with NO can proceed via two different pathways. In one pathway, it converts NO into NO_2 and leads to acetaldehyde and HO_2 (99.1%). In the other pathway, the reaction leads to nitrate formation (0.9%). The reaction of ethane with Cl also proceeds via the hydrogen abstraction pathway. With the exception of HCl rather than H_2O, its reaction products are same as the products of the reaction between ethane and OH (R11). In addition, the products from the existing reaction with chlorine and isoprene were modified to more explicitly track the fate of Cl and carbon from isoprene. The HCl and formyl chloride yields reflect the balance between hydrogen atom abstraction and addition pathways of 15% and 85% (Fan and Zhang; 2004). Formyl chloride serves as a surrogate for all products where chlorine is incorporated into a chlorocarbonyl after an addition reaction. Reaction of terpenes with Cl atoms is not included because the reaction products are too uncertain. Omitting the reaction may not greatly alter the fate of Cl atoms because Cl atoms react rapidly with all VOCs. For example, the global background for CH_4 of about 1.8 ppm (Oum et al., 1998) provides a significant "universal" sink for Cl atoms because Cl atoms react quite rapidly with CH_4.

The next major updates to the Tanaka et al. (2003b) work is the inclusion of new reactions that lead to the formation of chlorine radicals including OH oxidation of HCl (R4) and photolysis and oxidation of formyl chloride (R18 and R17). The new chemistry also includes both the gas-phase formation of $ClNO_2$ (R9) and its subsequent photolysis (R3) as described by (Atkinson et al., 2005). In total, the updated chlorine mechanism contains five sources of reactive gas-phase Cl: photolysis of Cl_2, HOCl, $ClNO_2$, and reaction of HCl with OH, and the self-reaction of ClO (R1-R5).

Normalized photolysis rates were used by Tanaka et al. (2003b). In the updated chlorine chemistry, photolysis rates, J, (min^{-1}) are directly calculated using the following general equation (Finlayson-Pitts and Pitts, 2000):

$$J = \int_{\lambda_1}^{\lambda_2} \sigma(\lambda)\Phi(\lambda)F(\lambda)d\lambda \qquad \text{(Equation 1)}$$

where, is $\sigma(\lambda)$ the absorption cross section (cm^2 $molecule^{-1}$), $\phi(\lambda)$ is the quantum yield (molecules $photon^{-1}$), $F(\lambda)$ is the actinix flux (photons cm^2 min^{-1}), λ is the wavelength (nm). Quantum yield and absorption cross-section data from the recent IUPAC recommendations are used in the mechanism (Atkinson et al., 2005). Photolysis of $ClNO_2$ can produce Cl and NO2 in the presence of sunlight (R3).

Finally, rate constants for several reactions described by Tanaka et al. (2003b), have been updated to meet the latest recommendations of IUPAC (Atkinson et al., 2005): the reaction of Cl with O_3 (R5); the reaction of ClO with NO and HO_2 (R7-R8); the reaction of ethane and Cl (R13).

Chlorine chemistry can affect O_3 primarily via two competing pathways that consume and produce O_3. It can directly consume O_3 via R5. It can also affect O_3 via reactions initiated by Cl and VOCs. Chlorine chemistry can enhance the oxidation of VOCs which then can produce additional peroxy radicals (HO_2 and RO_2). The reaction of NO with HO_2 and RO_2 converts NO into NO_2 and cause O_3 production when NO_2 is photolyzed (Finlayson-Pitts and Pitts, 2000):

$HO_2 + NO \rightarrow HO + NO_2$ (R26)

$NO_2 + hv \rightarrow NO + O(^3P)$ (R27)

$\underline{O(^3P) + O_2 \rightarrow O_3}$ (R28)

$HO_2 + O_2 \rightarrow OH + O_3$ (R29: net result of R26 to R28)

$RO_2 + NO \rightarrow RO + NO_2$ (R30)

If additional O_3 production via reactions R26 and R30 exceeds O_3 consumption via R5, O_3 will increase.

2.3 Heterogeneous reaction

Although $ClNO_2$ can be formed in the gas phase through reaction R9, the high nighttime $ClNO_2$ concentrations observed in recent field campaigns are predominantly formed from reactions of N_2O_5 on particle surfaces. Current versions of CMAQ treat this heterogeneous N_2O_5 chemistry as producing only nitric acid (R31).

$N_2O_5(g) + H_2O(aq) \rightarrow 2*HNO_3\ (g)$ (R31)

CMAQv5.0 calculates the rate constant of reaction R31 ($k_{N_2O_5,het}$) on fine PM using equation (2).

$$k_{N_2O_5,het} = \left(\frac{\tilde{d}}{2D} + \frac{4}{\bar{c}\gamma}\right)^{-1} A \qquad \text{Equation (2)}$$

In equation 2, $\tilde{d}$represents the effective diameter, D represents the diffusivity of N_2O_5 in air (as a function of temperature and pressure), $\bar{c}$ is the mean molecular velocity of N_2O_5 (a function of temperature), A is the aerosol

surface area concentration, and γ is the reactive uptake coefficient defined as the probability that a collision between an N_2O_5 molecule colliding with an aerosol particle will result in a reaction. The derivation of this equation is discussed in more detail elsewhere (Jacob, 2000). The CMAQ model calculates γ_{N2O5} as a complex function of temperature, relative humidity, particle composition, and phase state (Davis et al., 2010).

The recent studies of Bertram and Thornton (2009) and Roberts et al. (2009) show that when particles contain chloride, $ClNO_2$ is also formed as a product (R32-R35).

$N_2O_5(g) \leftrightarrow NO_3^-(aq) + NO_2^+(aq)$ (R32)

$NO_3^-(aq) + H^+(aq) \rightarrow HNO_3(g)$ (R33)

$NO_2^+(aq) + OH^-(aq) \rightarrow HNO_3(g)$ (R34)

$NO_2^+(aq) + Cl^-(aq) \rightarrow ClNO_2(g)$ (R35)

$N_2O_5 + H_2O \rightarrow Y*(HNO3 + ClNO_2) + 2*(1 - Y)\ HNO_3$ (R36: net result of R32-R35)

The yield of $ClNO_2$ (Y) represents the likelihood of $NO_2^+(aq)$ reacting via R34 versus R35. This yield depends on the amount of molar concentrations of $Cl^-(aq)$ present in the particle and has been parameterized by Bertram and Thornton (2009) and Roberts et al. (2009). Both suggested a similar correlation (Eq 3):

$$Y = \frac{1}{1+\frac{k_{34}[H_2O(l)]}{k_{35}[Cl^-]}} \quad \text{(Equation 3)}$$

where $H_2O(l)$ = particle liquid water and Cl^- = particulate chloride. Bertram and Thornton (2009) derived a value of 483 for k_{35}/k_{34} while Roberts et al. (2009) derived a value of 485 for k_{35}/k_{34}. The formation of $ClNO_2$ in place of HNO_3 has implications for the reactive nitrogen budget since HNO_3 deposits quickly while $ClNO_2$ does not. Consequently, an increase in Y leads to increased availability of NO_x which participates in photochemical O_3 production outlined in Eqs 26-30.

Bertram and Thornton (2009) also suggested that the presence of particulate chloride can alter γ_{N2O5} and developed a correlation (Eq 4).

$$\gamma_{N_2O_5} = A\,k'_{31f}\left(1 - \frac{1}{\left(\frac{k_{34}[H_2O(l)]}{k_{32b}[NO_3^-]}\right)+1+\left(\frac{k_{35}[Cl^-]}{k_{32b}[NO_3^-]}\right)}\right) \quad \text{(Equation 4)}$$

where $H_2O(l)$ = particle liquid water, NO_3^- = particulate nitrate, Cl^- = particulate chloride, $k_{34}/k_{32b} = 6\text{x}10^{-2}$, $k_{35}/k_{32b} = 29$, $A = 3.2\text{x}10^{-8}$, and k'_{31f} is calculated as follows:

$$k'_{31f} = \beta - \beta e^{|-\delta[H_2O(l)]|} \quad \text{(Equation 5)}$$

where, $\beta = 1.15\text{x}10^{-6}$, and $\delta = 1.3\text{x}10^{-1}$ (Bertram and Thornton, 2009).

In this study, we replace R31 with R36 in CMAQ. The yield and reactions rates are calculated separately for coarse and fine particles and use the chloride and water contents in the appropriately-size particles. The yield for R36 is calculated with Eq 3 on both fine and coarse particles. Reactive uptake (γ_{N2O5}) is calculated based on Davis et al. (2010) for fine particles (as is done in the base version of CMAQ) and is calculated based on Eq 4 (using k_{34}/k_{33} from Bertram and Thornton (2009)) for coarse particles. To conserve mass of chlorine, particulate chloride mass is reduced by the amount of chlorine in $ClNO_2$ formed via the heterogeneous reaction on fine as well as coarse particles. If no particulate chloride is present, then Y=0 according to Eq 3 and no $ClNO_2$ is formed.

2.4 Simulation details

To evaluate the impacts of heterogeneous $ClNO_2$ formation on air quality, two different simulations were completed. The base simulation was conducted with Y = 0. Thus, only gas-phase reactions produced $ClNO_2$. The other simulation was conducted with yield calculated from Eq 3 so that the heterogeneous hydrolysis of N_2O_5 produces HNO_3 and $ClNO_2$. Both the gas-phase and heterogeneous reactions produced $ClNO_2$. Differences in the results obtained with the two simulations are attributed to the heterogeneous production of $ClNO_2$.

3.0 Results and Discussion

3.1 Model performance without heterogeneous $ClNO_2$ production

Model performance statistics for the base simulation without the heterogeneous $ClNO_2$ production for 8-hr O_3 and daily mean $PM_{2.5}$ are shown in Tables 2 and 3. Ambient monitoring data from the United States Environmental Protection Agency's Air Quality System (AQS) are used to evaluate 8-hr O_3. We show statistics both for all 8-hr max O_3 concentrations and for only observed values above 65 ppbv to show how the model performs during high pollution episodes. The model captures observed 8-hr O_3 data reasonably well. Model mean values are slightly greater than the observed values both in February and September. Ambient monitoring data from the AQS are used to evaluate daily mean $PM_{2.5}$ levels measured by the Federal Referenced Method (FRM). In addition, daily mean $PM_{2.5}$ levels from the Interagency Monitoring of PROtected Visual Environments (IMPROVE) network and the Chemical Speciation Network (CSN) are also used to evaluate the model results. The model captures observed $PM_{2.5}$ levels at all monitoring networks both in February and September. Model performance statistics are similar to or better than those for the previous versions of the model (Eder and Yu, 2006; Appel et al., 2007; Foley et al., 2010).

Predicted mean fine-particulate chloride levels in the base simulation are shown in Figure 1(a-b). Fine particulate chloride concentrations are highest in coastal areas and the mid-west. In addition, fine particulate chloride is present in the entire eastern half of the United States in February and Idaho in September. The fine particulate chloride in the eastern United States is largely derived from anthropogenic sources (mostly fugitive dust), while fine particulate chloride in the coastal areas comes mostly from sea salt. The high modeled levels in Idaho in September are due to particulate chloride emissions from a large wildfire. While the magnitudes of predicted levels are greater in

September, predicted particulate chloride in February is present over a larger geographical area. Predicted mean coarse particulate chloride levels without the heterogeneous $ClNO_2$ production are shown in Figure 1(c-d).

Predicted fine particulate chloride levels averaged across all measurement sites in the United States are compared to the observed data from IMPROVE in Figure 1(e-f). With the exception of a few days in early February, average predictions are in good agreement with average observed data. Previous studies using the Tanaka et al. (2003b) chlorine chemistry and no $ClNO_2$ formation also showed reasonable performance of particulate chloride predictions. Kelly et al. (2010) compared CMAQ predictions to size resolved (both fine and coarse particles) particulate chloride observations from three coastal monitoring sites in Florida and reported good agreement between the model predictions and the observed data. Bhave and Appel (2009) compared CMAQ predictions to size resolved (both fine and coarse particles) particulate chloride observations from multiple monitoring sites in the United States and also reported good agreement. These results suggest model predicted fine and coarse particulate chloride levels are in good agreement with observed data and can be used to examine the impact of heterogeneous $ClNO_2$ production on air quality.

3.2 Impact of heterogeneous $ClNO_2$ chemistry on model performance statistics

The heterogeneous production of $ClNO_2$ marginally affects model performance statistics for daily maximum 8-hr O_3. For example, it changed the NMB from -20.2 % to -18.8% in February and 0.1% to 0.4% in September for observed values above 65 ppbv. These changes which are mapped in figure S1 show that improvements and degradations in model performances do not have a noticeable geographic pattern. The inclusion of heterogeneous $ClNO_2$ formation also changed NME both in February and September by similar margins.

Predicted total nitrate (TNO_3) are compared with observed data from the Clean Air Status and Trends Network (CASTNet). Predicted TNO_3 without the heterogeneous production are greater than the observed data with NMB of 61.1% in February and 89.5% in September. Previous studies also reported over-predictions of nitrate (Foley et al., 2010). The over-predictions may be partially due to the γ_{N2O5} parameterization used in the model. Brown et al. (2006) measured γ_{N2O5} values in the eastern United States and reported the values to be much lower than those derived from model based approaches. All current γ_{N2O5} parameterizations, available in the peer-reviewed literature, produce higher γ_{N2O5} values. The heterogeneous production of $ClNO_2$ reduced the NMB to 57.1% in February and 85.9% in September for TNO_3 in the CASTNet. The heterogeneous production of $ClNO_2$ reduced the NMB from 64.2% to 61.2% in February and 42.1% to 36.4% in September for aerosol nitrate in the IMPROVE. It also reduced the NMB from 44.8% to 41.7% in February and 67.7% to 60.5% in September for aerosol nitrate in the CSN. These improvements are shown in figures S2, S3, S4, and S5 and are most pronounced in the Eastern US in February where observed total nitrate concentrations are highest.

To evaluate the sensitivity of the model results to particulate chloride concentrations, two additional simulations were conducted with increased chlorine emissions [3.0 x (anthropogenic particulate chloride, Cl_2, HCl) emissions

used for the previous two simulations] for 10 days in February. One simulation was conducted without the heterogeneous production of $ClNO_2$ and the other simulation was conducted with the heterogeneous production of $ClNO_2$. The additional chlorine emissions further increased $ClNO_2$ and O_3 and further decreased TNO_3. They increased mean $ClNO_2$ by up to 0.43 ppb compared to the value of 0.3 ppbv with the normal emissions. They increased mean O_3 by up to 2.1 ppb compared to the value of 1.2 ppbv with the normal emissions. They increased mean O_3 in the northeast United States by 1.0-2.0 ppb while the normal emissions increased mean O_3 by 0.6-1.0 ppbv. They decreased mean TNO_3 by up to 1.2 $\mu g/m^3$ compared to the value of 0.9 $\mu g/m^3$ with the normal emissions. They decreased mean TNO_3 in the Mid-west by 0.4-0.6 $\mu g/m^3$ compared to the values of 0.1-0.3 $\mu g/m^3$ with the normal emissions. The impacts on $ClNO_2$, O_3 and TNO_3 were more pronounced with the enhanced emissions. Thus, the heterogeneous production of $ClNO_2$ can further increase O_3 and further lower TNO_3 predictions and improve the model performance statistics if adequate chlorides are present in the atmosphere. These results suggest that $ClNO_2$ formation is limited more by the presence of particulate chloride than by the abundance of N_2O_5.

3.3 Predicted Y, $ClNO_2$ levels, and comparison with observed $ClNO_2$

Predicted mean values of Y on fine and coarse particles with the heterogeneous $ClNO_2$ production are presented in Figure 2. As might be expected from Eq 3, calculated yield is largest in areas in which particulate chloride concentrations are highest. Modeled yields on fine particles reached values above 0.7 in many coastal and in-land areas. Yield values on coarse particles reached 1.0 over the Gulf and the Oceans and ranged between 0.1 and 0.8 in coastal and in-land areas. These modeled yields suggest that the presence of particulate chloride can efficiently activate the heterogeneous $ClNO_2$ production pathway throughout large areas of the United States.

Modeled mean $ClNO_2$ levels in the base simulation that included only the gas-phase formation pathway (no heterogeneous $ClNO_2$ production) are negligible (generally <0.5 pptv) and are not discussed further. Heterogeneous production enhanced $ClNO_2$ levels both in February and September. Predicted monthly mean and the hourly maximum $ClNO_2$ levels during the entire month with the heterogeneous production are presented in Figure 3. $ClNO_2$ formed where particulate chloride and NO_x concentrations are prevalent. The highest monthly mean predicted $ClNO_2$ was found in the Los Angeles area both in February (0.3 ppbv) and in September (0.5 ppbv). Mean $ClNO_2$ concentrations also reached moderate values of around 0.1 to 0.2 ppbv in portions of the Northeast during both September and February. While predicted values reached higher concentrations in September, predicted levels are more spatially distributed in February. The maximum hourly predicted value in February reached to almost 3.0 ppbv in Los Angeles and 2.0 ppbv in Midwest. High hourly $ClNO_2$ concentrations in September were found in Idaho (4.5 ppbv maximum) and in Los Angeles (4.0 ppbv maximum). Predicted $ClNO_2$ levels were consistently high in Los Angeles both in February and September. It increased $ClNO_2$ in coastal areas due to the sea-salt emissions and the Mid-west due to anthropogenic chloride emissions. In addition, it enhanced $ClNO_2$ over the eastern half of the United States in February due to anthropogenic chloride emissions and Idaho due to chloride emissions from the forest fires in September.

Ambient $ClNO_2$ levels are not routinely measured; these measurements are conducted only in specialized field campaigns. To our knowledge, four sets of measurements have been published in the peer-reviewed literature. A qualitative comparison of predicted $ClNO_2$ levels with these measurements is presented in Table 4. Osthoff et al. (2008) measured $ClNO_2$ in Houston in 2006 and reported a peak value of about 1,200 pptv. Predicted peak $ClNO_2$ in Houston reached to 2,000 pptv in February and 1,500 pptv in September. Thornton et al. (2010) reported a peak value of 450 pptv in Boulder, Colorado in February 2009. Predicted peak value in Boulder was 300 pptv in February and 200 pptv in September. Mielke et al. (2011) reported a peak $ClNO_2$ value of 250 pptv in Calgary, Canada in April 2010. Predicted peak value in Calgary reached to 500 pptv in February and 300 pptv in September. Mielke et al. (2010) reported a peak value of 2,550 pptv in Los Angeles, California in June 2010. Predicted peak value in Los Angeles reached to 2,700 pptv in February and 4,000 pptv in September. Predicted levels are similar to the observed values reported in the literature. Based on these comparisons, the model parameterizations of yield and γ_{N2O5} along with our emissions of NO_x and gas and particle-phase chlorine compounds appear to do a reasonable job of replicating the chemistry that leads to $ClNO_2$ production.

3.4 Impact of the heterogeneous $ClNO_2$ production on selected gaseous and particle species

3.4.1 Monthly mean concentrations

Monthly mean O_3 levels in the base simulation and changes due to the heterogeneous production are presented in Figure 4. Monthly mean O_3 levels between 30 and 50 ppbv in February and between 40 and 65 ppbv in September were modeled over most areas in the United States. The heterogeneous $ClNO_2$ production enhanced monthly mean O_3 by a maximum of 1.3 ppbv in February and 1.4 ppbv in September. On a percentage basis, the enhancement ranged up to 4% and 3% in February and September, respectively. Enhancements in February occurred over a larger geographic area than those in September. Predictions of $ClNO_2$ occurred over a wider area in February; consequently enhancements also occurred over a larger geographic area. Although not shown here, the heterogeneous $ClNO_2$ production enhanced mean HO_2 and RO_2 by a few percent. These radicals increased primarily due to the oxidation of VOCs by Cl which is produced via the photolysis of $ClNO_2$. Enhancements of O_3 in the heterogeneous $ClNO_2$ formation simulation were due both to the increased HO_2 and RO_2 radicals and due to the increased availability of NO_2.

Monthly mean total nitrate (TNO_3) levels in the base simulation and changes due to the heterogeneous production are presented in Figure 5. Here we define TNO_3 as the sum of HNO_3 and fine and coarse particle nitrate. Mean TNO_3 levels of more than 4.0 $\mu g/m^3$ are predicted over most of the eastern United States and southern California in February and over parts of Mid-west, southern United States, and southern California in September. The activation of the heterogeneous $ClNO_2$ pathway reduced the production of HNO_3 via the N_2O_5 hydrolysis which then decreased TNO_3 both in February and September. The mean decreases in February were up to 0.8 $\mu g/m^3$ while the decrease in September reached to 2.0 $\mu g/m^3$. On a percentage basis, the reductions were up to 11% and 21% in February and

September, respectively. Both high nitrate concentrations and large nitrate decreases covered a broader area in February than in September.

The heterogeneous $ClNO_2$ production also enhanced sulfate by <0.1 $\mu g/m^3$, decreased ammonium by <0.3 $\mu g/m^3$, and increased anthropogenic as well as biogenic secondary organic aerosols by <0.003 $\mu g/m^3$. These changes are due to shifts in the radical budget and NO_x availability and are not discussed further in this paper.

3.4.2 Day-to-day variation

Several areas were identified as having high modeled $ClNO_2$ concentrations in section 3.3. Here we examine the temporally-resolved changes in $ClNO_2$, O_3, and TNO_3 in those areas. Time series of the changes in $ClNO_2$, O_3, and TNO_3 due to the heterogeneous production in Los Angeles, Indiana, and Idaho are shown Figure 6. These values are averaged over each representative region and since $ClNO_2$ formation chemistry can occur in localized areas, this analysis does not show the maximum impact of that chemistry. Figure 6 shows that $ClNO_2$ concentrations increase every day in Los Angeles in both February and September. Predicted increases in $ClNO_2$ in February are lower than those in September in Los Angeles. Nightly concentrations averaged over the Los Angeles area range 0.15 ppbv to above 1.0 ppbv. These fairly routine $ClNO_2$ episodes are due to the constant source of particulate chloride from sea-salts and NO_x from mobile sources. Ozone enhancements and TNO_3 decrease due to the $ClNO_2$ chemistry are predicted daily in Los Angeles and range from 0.3 to 3 ppb for O_3 and from 0.1 to 4.0 $\mu g/m^3$ for TNO_3. Anthropogenic particulate chloride emissions are responsible for the chlorine available for heterogeneous production in Indiana and enhanced $ClNO_2$ and O_3, and decreased TNO_3 on most days in February. Chloride and NO_x emissions from a large wildfire in Idaho activated the heterogeneous production and increased $ClNO_2$ and O_3 up to 1 ppbv and 2.5 ppbv respectively and decreased TNO_3 by up to 2.5 $\mu g/m^3$ over a large portion of Idaho. The wildfire was active only during the first part in September and consequently the heterogeneous production during the second part in September is negligible. Thus, the heterogeneous $ClNO_2$ production can be active on most days in some areas while it can be activated by sporadic events such as wildfires or large industrial emissions in other areas.

3.4.3 Diurnal variation of the impact

Diurnal changes in $ClNO_2$, O_3, TNO_3 at Los Angeles, Indiana, and northeastern United States due to the heterogeneous production of $ClNO_2$ are shown Figure 7. Again, these changes are averaged over each representative area. $ClNO_2$ increased during the course of night, reached peak levels in the early morning and then decreased due to the photolysis and dropped to its lowest level in the afternoon. The peak $ClNO_2$ levels in February occurred somewhat later in the morning than those in September due to the lower photolysis rate and late sun rise. The modeled diurnal pattern of $ClNO_2$ agrees well with observed profile reported by Thornton et al. (2010). The O_3 enhancement started in the morning and reached a peak value in the afternoon and then decreased. The time of peak O_3 increase varied by season; O_3 enhancements reached their peak around noon September and later in the afternoon in February. So even though $ClNO_2$ photolysis released Cl radicals and NO_2 in the first several hours after sunrise, these model simulations predict that its effect on O_3 continues well into the day meaning that $ClNO_2$ production will have a noticeable impact of 8-hr daily maximum O_3, the regulatory metric used to identify areas in violation with

national air quality standards. The decrease in TNO_3 followed the same diurnal pattern as the changes in $ClNO_2$ since the decrease of HNO_3 is a direct result of the heterogeneous N_2O_5 chemistry following the pathway of $ClNO_2$ formation (R35) rather than HNO_3 production (R34). Similar diurnal pattern of the changes in $ClNO_2$, O_3, TNO_3 were observed in other areas.

3.4.4 Impact on daily maximum 8-hr O_3

Predicted mean 8-hr O_3 in the base simulation and enhancements due to the heterogeneous production are presented in Figure 8. Predicted mean 8-hr O_3 without the heterogeneous production are greater than 46 ppbv in most of the United States in September while predicted values are lower than 46 ppbv in February. The heterogeneous production enhanced the monthly mean 8-hr O_3 by up to 1.7 ppbv in February and 1.9 ppbv in September. On a percentage basis, the enhancement ranged up to 4% and 3% in February and September, respectively. The largest monthly mean impact occurred in Los Angeles both in February and September. The largest enhancement in daily maximum 8-hr O_3 in any grid-cell was 13.3 ppb in February and 6.6 ppbv in September. On a percentage basis, the largest enhancement in daily maximum 8-hr O_3 in any grid-cell was 43% in February and 10% in September. Although mean enhancements in maximum 8-hr O_3 are modest, impacts on specific days can be quite large.

3.5 Impact on the composition of total reactive nitrogen (NO_Y)

The mean $ClNO_2$:NO_Y ratios without the heterogeneous $ClNO_2$ production are negligible (< 0.001). Heterogeneous $ClNO_2$ production increased $ClNO_2$:NO_Y ratios up to 0.04 in February and 0.03 in September. As TNO_3 concentrations decreased with heterogeneous $ClNO_2$ production, so did their contribution to NO_Y. While the mean $ClNO_2$:NO_Y ratios were only 0.03-0.04, the maximum hourly $ClNO_2$:NO_Y ratios are much greater and reached 0.34 in February and 0.17 in September. The contribution of $ClNO_2$ to NO_Y was generally greater in February than in September; thus, the ratio was also higher in February.

3.6 Impact of γ_{N2O5} parameterization on model predictions

The presence of particulate chloride can increase γ_{N2O5} value as described by Bertram and Thornton (2009). However particulate chloride is not explicitly accounted for in the γ_{N2O5} which is described by Davis et al. (2010) and used in the current version of CMAQ. The Davis et al. (2010) parameterization was also used to calculate the heterogeneous reaction rate on fine particles in this work. To evaluate the sensitivity of the model results to γ_{N2O5}, two additional simulations were completed for a 10-day period in each month. The first simulation employed γ_{N2O5} (Eq-4) of Bertram and Thornton (2009) on both fine and coarse particles and used Y= 0. The second simulation employed γ_{N2O5} of Bertram and Thornton (2009) on both fine and coarse particles with Y calculated using Eq 3. The differences in results obtained with the two simulations are compared to those obtained with the previous two simulations employing γ_{N2O5} of Davis et al. (2010) on fine particles and γ_{N2O5} of Bertram and Thornton (2009) on coarse particles. While enhancements in hourly O_3 obtained with the two γ_{N2O5} varied occasionally by 1-2 ppbv, the enhancements in mean 8-hr O_3 obtained with the two γ_{N2O5} did not differ significantly (<0.2 ppb). The decreases in hourly as well as mean TNO_3 obtained with γ_{N2O5} of Bertram and Thornton (2009) on both fine and coarse particles

were greater than those obtained with the modeling simulations described in the main portion of this paper. The additional mean decreases ranged up to 0.4-1.4 $\mu g/m^3$. Thus, the use of γ_{N2O5} of Bertram and Thornton (2009) on both fine and coarse particles can further reduce TNO_3 without further enhancement of O_3.

4.0 Summary

Heterogeneous $ClNO_2$ chemistry is successfully implemented into the CMAQ model along with a comprehensive inventory of chlorine and reactive nitrogen emissions. While the homogeneous production of $ClNO_2$ is negligible, the heterogeneous production can enhance $ClNO_2$ in coastal areas, the eastern half of the United States, and Idaho. Sea-salt derived particulate chloride enhances $ClNO_2$ in coastal areas while anthropogenic particulate chloride enhances $ClNO_2$ in the eastern half of the United States and chloride from forest fires enhances $ClNO_2$ in Idaho. Mean $ClNO_2$ levels increase by up to 0.3 ppbv in February and 0.5 ppbv in September though the maximum hourly values are much greater.

Predicted $ClNO_2$ enhances monthly mean 8-hr O_3 modestly. It can, however, decrease mean TNO_3 by larger margins and improve model performance statistics. Predicted $ClNO_2$ reaches its peak level in the early morning while the O_3 enhancement starts in the morning and reaches a peak value in the afternoon. The impact of the heterogeneous production occurs over a larger geographical area in February. The heterogeneous production of $ClNO_2$ changes the composition of NO_Y; predicted $ClNO_2$ can account for up to 3-4% of the monthly mean NO_Y but up to 34% of NO_y in some localized episodes.

The results of this study compare favorably to the findings of Simon et al. (2009) who reported that the heterogeneous $ClNO_2$ production can increase daily maximum 8-hr O_3 in Houston by up to 1.5 ppbv. While the heterogeneous $ClNO_2$ production, in this study, enhances monthly mean 8-hr O_3 by less than 0.2 ppbv in Houston, it enhanced the daily maximum 8-hr O_3 by levels similar to those reported by Simon et al. (2009). It should be noted that Simon et al. (2009) used 4-km grid resolution and this study uses 12-km grid resolution. Since the modeling domain covers the entire United States, larger grid resolution are used in this study. Emissions of NO_x and VOCs used by Simon et al. (2009) are also different than those used in this study. One large improvement over the modeling formulation presented in that work is that this modeling uses generalized parameterizations for reactive uptake and $ClNO_2$ yield while Simon et al. (2009) relied on local measurements to create fixed values for those variables. Our new model formulation has allowed for the investigation of the effects $ClNO_2$ chemistry over the entire continental United States and over multiple seasons. Our predicted yields in Houston are lower than the fixed 0.75 value used by Simon et al. (2009). Results of this study suggest that the effect of $ClNO_2$ production on air quality is more pronounced in several areas in the United States than it is in Houston. Field campaigns can be planned in these areas to validate the findings of this study.

Disclaimer

Although this paper has been reviewed by EPA and approved for publication, it does not necessarily reflect EPA's policies or views.

References

Appel, K. W., Gilliland, A. B., Sarwar, G., and Gilliam, R. C.: Evaluation of the Community Multiscale Air Quality (CMAQ) model version 4.5: Sensitivities impacting model performance, Part I-Ozone, Atmospheric Environment, 41, 9603–9615, 2007.

Atkinson, R., and Coauthors: Summary of evaluated kinetic and photochemical data for atmospheric chemistry - IUPAC subcommittee on gas kinetic data evaluation for atmospheric chemistry, 2005. Available at http://www.iupac-kinetic.ch.cam.ac.uk/index.html.

Bhave, P. V. and Appel. K.W.: Evaluation of the CMAQ Model for Size-Resolved PM Composition, 8th Annual CMAS Models-3 Users' Conference, October 19-21, 2009, UNC-Chapel Hill, NC. Available at http://www.cmascenter.org/conference/2009/agenda.cfm

Bertram, T.H. and Thornton J.A.: Toward a general parameterization of N_2O_5 reactivity on aqueous particles: the competing effects of particle liquid water, nitrate and chloride, Atmos. Chem. Phys., 9, 8351-8363, 2009.

Binkowski, F.S. and Roselle, S.J.: Community Multiscale Air Quality (CMAQ) model aerosol component, I: Model description, J. Geophys. Res., 108(D6): 4183, doi: 10.1029/2001JD001409, 2003.

Brown, S. S., Ryerson, T. B., Wollny, A. G., Brock, C. A., Peltier, R., Sullivan, A. P., Weber, R. J., Dube, W. P., Trainer, M., Meagher, J. F., Fehsenfeld, F. C., and Ravishankara, A. R.: Variability in nocturnal nitrogen oxide processing and its role in regional air quality, Science, 311, 67–70, 2006.

Byun, D., and Schere, K. L.: Review of the governing equations, computational algorithms, and other components of the Models-3 Community Multiscale Air Quality (CMAQ) modeling system, Applied Mechanics Reviews, 59, 51–77, 2006.

Chang, S., McDonald-Buller, E. C., Kimura, Y., Yarwood, G., Neece, J., Russel, M., Tanaka, P., and Allen, D.: Sensitivity of urban ozone formation to chlorine emission estimates, Atmospheric Environment, 36, 4991-5003, 2002.

Chang, S. and Allen, D. T.: Atmospheric chlorine chemistry in Southeast Texas: Impacts on ozone formation and control, Environmental Science & Technology, 40, 251-262, 2006.

Davis, J. M., Bhave, P. V., and Foley, K. M.: Parameterization of N2O5 reaction probabilities on the surface of particles containing ammonium, sulfate, and nitrate, Atmos. Chem. Phys., 8, 5295–5311, 2008,

Eder,.B. and Yu, S.: A performance evaluation of the 2004 release of Models-3 CMAQ, Atmospheric Environment, 40, 4811–4824, 2004.

Fan, J. and Zhang, R.: Atmospheric Oxidation mechanism of isoprene, Environ. Chem. 1, 140-149, 2004.

Finlayson-Pitts, B.J., Ezell, J.J., Pitts Jr., J.N.: Formation of chemically active chlorine compounds by reactions of atmospheric NaCl particles with gaseous N_2O_5 and $ClONO_2$, Nature, 337, 241-244, 1989.

Finlayson-Pitts, B.J., Pitts Jr., J. N.: Chemistry of the Upper Lower Atmosphere, Theory, Experiments and Applications, Academic Press, San Diego, 2000.

Foley, K. M., Roselle, S.J., Appel, K.W., Bhave, P.V., Pleim, J.E., Otte, T.L., Mathur, R., Sarwar, G., Young, J.O., Gilliam, R.C., Nolte, C.G., Kelly, J.T., Gilliland, A.B., Bash, J.O.: Incremental testing of the Community Multiscale Air Quality (CMAQ) modeling system version 4.7, Geosci. Model Dev., 3, 205–226, 2010.

Gery, M.W., Whitten, G.Z.,Killus, J.P., and Dodge, M.C.: A photochemical kinetics mechanism for urban and regional scale computer modeling. J. Geophys. Res., 94(D10): 12925-12956, 1989.

Houyoux, M. R., Vukovich, J. M., Coats Jr., C. J., Wheeler, N. M., Kasibhatla, P. S.: Emission inventory development and processing for the seasonal model for regional air quality (SMRAQ) project, J. of Geophys. Res. 105, 9079–9090, 2000.

Jacob, D.J.: Heterogeneous chemistry and tropospheric ozone, Atmospheric Environment, 34, 2131-2159, 2000.

Kelly, J. T., Bhave, P. V., Nolte, C. G., Shankar, U., and Foley, K.M.: Simulating emission and chemical evolution of coarse seasalt particles in the Community Multiscale Air Quality (CMAQ) model, Geosci. Model Dev. 3, 257-273, 2010.

Knipping, E.M. and Dabdub, D.: Impact of chlorine emissions from sea-salt aerosol on coastal urban ozone, Environmental Science & Technology, 37, 275-284, 2003.

Mielke, L.H, Flynn, J.H., Grossberg, N., Lefer, B.L., Veres, P.R., Roberts, J.M., Froyd, K.D., Cochran, A.K., and Osthoff, H.D.: Quantification and analysis of CalNex-LA 2010, American Geophysical Union, Fall Meeting 2010, San Francisco, California. Available at http://adsabs.harvard.edu/abs/2010AGUFM.A21C0118M.

Mielke, L.H, Furgeson, A., and Osthoff, H.D.: Observation of $ClNO_2$ in a mid-continental urban environment, Environmental Science & Technology, 45(20), 8889-8896, 2011.

Osthoff, H.D., Roberts J.M., Ravishankara, A.R., Williams, E.J., Lerner, B.M., Sommariva, R., Bates, T.S., Coffman D., Quinn P.K., Dibb, J.E., Stark H., Burkholder J.B., Talukdar, R.K., Meagher, J.M., Fehsenfeld F.C., and Brown, S.S.:

High levels of nitryl chloride in the polluted subtropical marine boundary layer, Nature Geoscience, 1, 324 – 328, 2008.

Oum, K.W., Lakin, M.J., DeHaan, D.O., Brauers, T., and Finlayson-Pitts, BJ.: Formation of molecular chlorine from the photolysis of ozone and aqueous sea-salt particles, Science, 279, 74-77, 1998.

Reff, A., Bhave, P. V., Simon, H., Pace, T. G., Pouliot, G. A.,Mobley, J. D., and Houyoux, M.: Emissions inventory of $PM_{2.5}$ trace elements across the United States, Environ. Sci. Technol.,43(15), 5790–5796, 2009.

Roberts, J. M., Osthoff, H.D., Brown, S.S., Ravishankara, A.R., Coffman, D., Quinn, P. and Bates, T.: Laboratory studies of products of N2O5 uptake on Cl- containing substrates, Geophysical Research Letters, *36*(L20808), 10.1029/2009GL040448, 2009.

Sarwar, G. and P. Bhave: Modeling the effect of chlorine emissions on atmospheric ozone across the eastern United States, *J.* of Appl. Meteo. and Clim., 46, 1009-1019, 2007.

Sarwar, G., Luecken, D., Yarwood, G., Whitten, G., Carter, B.: Impact of an updated Carbon Bond mechanism on air quality using the Community Multiscale Air Quality modeling system: preliminary assessment, Journal of Applied Meteorology and Climatology, 47, 3-14, 2008.

Sarwar, G., Appel, W., Carlton, A. G., Mathiur, R., Schere, K., Zhang, R., and Majeed, M.: Impact of a new condensed toluene mechanism on air quality model predictions in the US, Geosci. Mod. Dev.,*4, 1-11, 2011.*

Schwede, D., Pouliot, G., and Pierce, T.: Changes to the biogenic emissions inventory system version 3 (BEIS3), 4th Annual CMAS Models-3 Users' Conference, September 26-28, 2005, UNC-Chapel Hill, NC. Available at http://www.cmascenter.org/html/2005_conference/abstracts/2_7.pdf

Simon, H., Kimura, Y., McGaughey, G., Allen, D.T., Brown, S.S., Osthoff, H.D., Roberts, J.M., D. Byun, D., and Lee, D.: Modeling the impact of $ClNO_2$ on ozone formation in the Houston area, J. Geophys. Res., 114, D00F03, doi:10.1029/2008JD010732, 2009.

Smith, J.D., DeSain, J.D., Taatjes, C.A.: Infrared laser absorption measurements of HCl(v=1) production in reactions of Cl atoms with isobutane, methanol, acetaldehyde, and toluene at 295 K, Chemical Physics Letter, 366, 417-425, 2002.

Tanaks, P.L., Riemer, D.D., Chang, S.H, Yarwood, G., McDonald-Buller, E.C., Apel, E.C., Oralando, J.J., Silva, P.F., Jimenez, J.L., Canagaratna, M.R., Neece, J.D., Mullins, C.B., Allen, D.T.: Direct evidence for chlorine-enhanced urban ozone formation in Houston, Texas, Atmospheric Environment, 37, 1393-1400, 2003a.

Tanaka, P., Allen, D. T., McDonald-Buller, E.C., Chang, S., Kimura, Y., Mullins, C.B., Yarwood, G., and Neece, J.D.: Development of a chlorine mechanism for use in the carbon bond IV chemistry model, Journal of Geophysical Research, 08, D4, 4145, 6-1:13, 2003b.

Thornton, J.A., Kercher J.P., Riedel T.P., Wagner N.L., Cozic J., Holloway J.S., Dube W.P, Wolfe G.M., Quinn P.K., Middlebrook A.M., Alexander B., and Brown S.S.: A large atomic chlorine source inferred from mid-continental reactive nitrogen chemistry, Nature, 464, 271-274, 2010.

Yarwood, G., Rao, S., Yocke, M., and Whitten, G.: Updates to the Carbon Bond Chemical Mechanism: CB05. Final Report to the US EPA, RT-0400675, 2005. Available at www.camx.com.

Yu, S., Dennis, R.L., Bhave, P.V., Eder, B.K.: Primary and secondary organic aerosols over the United States: estimates on the basis of observed organic carbon (OC) and elemental carbon (EC), and air quality modeled primary OC/EC ratios, Atmospheric Environment, 38, 5257–5268, 2004.

Wallington, T.J., Skewes, L.M., Siegl, W.O.: Kinetics of the gas phase reaction of chlorine atoms with a series of alkenes,alkynes and aromatic species at 295 K, J. Photochem. Photobiol. A, 45, 167-175, 1988.

Whitten, G. Z., Heo., G., Kimura, Y., McDonald-Buller, E., Allen, D., Carter, W.P.L., and Yarwood, G.: A new condensed toluene mechanism for Carbon Bond: CB05-TU, Atmospheric Environment, 44, 5346-5355, 2010.

Tables

Figures

improvements in model performance. All plots show comparisons at CASTNet monitoring sites during the month of September 2006.

Figure S4. Particulate NO_3 mean observed concentration (top), Particulate NO_3 mean bias in the simulation without heterogeneous $ClNO_2$ formation (middle) and change in absolute value of Particulate NO_3 mean bias with the implementation of $ClNO_2$ chemistry (bottom). Negative values in bottom plot denote degradations in performance and positive values denote improvements in model performance. All plots show comparisons at CASTNet, CSN, IMPROVE, and SEARCH monitoring sites during the month of February 2006.

Figure S5. Particulate NO_3 mean observed concentration (top), Particulate NO_3 mean bias in the simulation without heterogeneous $ClNO_2$ formation (middle) and change in absolute value of Particulate NO_3 mean bias with the implementation of $ClNO_2$ chemistry (bottom). Negative values in bottom plot denote degradations in performance and positive values denote improvements in model performance. All plots show comparisons at CASTNet, CSN, IMPROVE, and SEARCH monitoring sites during the month of September 2006.

Tables

Table 1: Reactions in the chlorine mechanism for use with the CB05 mechanism

No.	Reactants	Products	Rate Expression [a]	Ref
R1	Cl2	2*Cl	Photolysis	b
R2	HOCl	OH + Cl	Photolysis	b
R3	ClNO2	Cl + NO2	Photolysis	b
R4	OH + HCl	Cl + H2O	$6.58 \times 10^{-13} (T/300)^{1.16} e^{(-58/T)}$	c
R5	Cl + O3	ClO + O2	$2.3 \times 10^{-11} e^{(-200/T)}$	b
R6	ClO + ClO	0.3*Cl2 + 1.4*Cl + O2	1.63×10^{-14}	b
R7	ClO + NO	Cl + NO2	$6.4 \times 10^{-12} e^{(290/T)}$	b
R8	ClO + HO2	HOCl + O2	$2.7 \times 10^{-12} e^{(220/T)}$	b
R9	Cl + NO2	ClNO2	$k_o = 1.8 \times 10^{-31} (T/300)^{-2.0}$ $k_\infty = 1.0 \times 10^{-10} (T/300)^{-1.0}$ F = 0.6 and N = 1.0	b
R10	Cl + CH4	HCl + MEO2	$6.6 \times 10^{-12} e^{(-1240/T)}$	b
R11	Cl + ETHA	HCl + 0.991*ALD2 + 0.991*XO2 + 0.009*XO2N + HO2	$8.3 \times 10^{-11} e^{(-100/T)}$	b
R12	Cl + PAR	HCl + 0.87*XO2 + 0.13*XO2N + 0.11*HO2 + 0.06*ALD2 - 0.11*PAR + 0.76*ROR + 0.05*ALDX	5.00×10^{-11}	b
R13	Cl + ETH	FMCl + 2.0*XO2 + HO2 + FORM	1.07×10^{-10}	b
R14	Cl + OLE	FMCl + 0.33*ALD2 + 0.67*ALDX + 2.0*XO2 + HO2 - PAR	2.5×10^{-10}	b
R15	Cl + IOLE	0.3*HCl + 0.7*FMCl + 0.45*ALD2 + 0.55*ALDX + 0.3*OLE + 0.3*PAR + 1.7*XO2 + HO_2	3.5×10^{-10}	b
R16	Cl + ISOP	0.15*HCl + XO2 + HO2 + 0.85*FMCl + ISPD	4.3×10^{-10}	b,d
R17	OH + FMCl	Cl + CO + H2O	5.0×10^{-13}	b
R18	FMCl	Cl + CO + HO2	Photolysis	b
R19	Cl + FORM	HCl + HO2 + CO	$8.2 \times 10^{-11} e^{(-34/T)}$	b
R20	Cl + ALD2	HCl + C2O3	7.9×10^{-11}	b
R21	Cl + ALDX	HCl + CXO3	1.3×10^{-10}	b
R22	Cl + MEOH	HCl + HO2 + FORM	5.5×10^{-11}	b
R23	Cl + ETOH	HCl + HO2 + ALD2	$8.2 \times 10^{-11} e^{(45/T)}$	b
R24	Cl + TOL	HCl + 0.88*XO2 + 0.88*HO2 + 0.12*XO2N	6.1×10^{-11}	e
R25	Cl + XYL	HCl + 0.84*XO2 + 0.84*HO2 + 0.16*XO2N	1.2×10^{-10}	f

Note:
[a] First order rate constants are in units of sec^{-1}, second order rate constants are in units of cm^3 $molecule^{-1}$ sec^{-1}. Temperatures (T) are in Kelvin. Rate constants for reaction 7 is described by the falloff expression of the form $k=\{k_o[M]/(1+k_o[M]/k_\infty)\}$ F^Z, where $Z=\{(1/N)+\log_{10}[k_o\,[M]/k_\infty]^2\}^{-1}$, where [M] is the total pressure in molecules/cm^3, and k_o, k_∞, F, and N are indicated in table.

Ref: b = Atkinson et al., 2005; c=Keene et al., 2007; d=Fan and Zhang; 2004; e= Smith et al., 2002; f= Wallington et al., 1988.

Cl2 = molecular chlorine, Cl = atomic chlorine, HOCl = hypochlorous acid, ClNO2 = nitryl chloride, HCl = hydrochloric acid, OH = hydroxyl radical, O2 = oxygen, O3 = ozone, ClO = chlorine oxide, NO = nitric oxide, NO2 = nitrogen dioxide, H2O = water vapor, HO2 = hydroperoxy radical, FMCl = formyl chloride, CO = carbon monoxide, CH4 = methane, ETHA = ethane, MEO2 = methylperoxy radical, PAR = paraffin carbon bond, XO2 = NO-to-NO_2 operator, XO2N = NO-to-nitrate operator, FORM = formaldehyde, ALD2 = acetaldehyde, ALDX = propionaldehyde and higher aldehydes, OLE = terminal olefinic carbon bond, IOLE = internal olefinic carbon bond, ETH = ethene, ISOP = isoprene, ISPD = isoprene product, MEOH = methanol, ETOH=ethanol, C2O3 = acetylperoxy radical, CXO3 = higher acylperoxy radicals, ROR = secondary organic oxy radical, TOL = toluene, XYL = xylene. The chlorine mechanism adds seven chemical species to CB05.

Table 2: Model performance statistics for 8-hr O_3

	AQS		AQS (obs > 65 ppbv)	
	February	September	February	September
Metric	8-hr O_3	8-hr O_3	8-hr O_3	8-hr O_3
Number of observations	14,873	20,019	22	912
Mean modeled (ppbv)	39.5	49.8	55.0	73.6
Mean observed (ppbv)	36.4	40.5	69.0	73.7
Median modeled (ppbv)	40.8	48.8	55.8	72.1
Median observed (ppbv)	37.1	39.2	68.3	70.8
NMB(%)	8.5	22.9	-20.2	-0.1
NME(%)	17.5	26.4	20.2	11.8
MB(ppb)	3.1	9.2	-14.0	-0.1
ME (ppb)	6.4	10.7	14.0	8.7

NMB = Normalized Mean Bias, NME = Normalized Mean Error, ME = Mean Error, MB = Mean Bias

Table 3: Model performance statistics for daily mean $PM_{2.5}$

	AQS FRM Sites		IMPROVE		CSN	
	February	September	February	September	February	September
Metric	Daily mean $PM_{2.5}$	Daily mean $PM_{2.5}$	Daily mean $PM_{2.5}$	Daily mean $PM_{2.5}$	Daily mean $PM_{2.5}$	Daily mean $PM_{2.5}$
Number of observations	9,553	5,998	1,348	831	949	628
Mean modeled ($\mu g/m^3$)	15.2	11.9	5.7	5.3	17.1	12.0
Mean observed ($\mu g/m^3$)	11.6	9.7	4.4	5.3	11.0	9.4
Median modeled ($\mu g/m^3$)	12.7	10.4	3.3	3.5	14.4	11.0
Median observed ($\mu g/m^3$)	9.8	8.3	2.9	4.0	11.0	8.8
NMB(%)	31.1	22.8	33.2	0.0	28.0	28.1
NME(%)	52.6	38.9	56.1	41.7	51.8	45.0
MB($\mu g/m^3$)	3.8	2.2	1.4	0.0	3.8	2.6
ME ($\mu g/m^3$)	6.1	3.8	2.4	2.2	6.9	4.2

FRM = Federal Reference Method

Table 4: A comparison of predicted nitryl chloride with observed data

Measurement location	**Measurement time period**	**References**	**Peak measurement value (pptv)**	**Peak prediction in February (pptv)**	**Peak prediction in September (pptv)**
Houston, Texas	8/30 – 9/8, 2006	Osthoff et al., 2008	1,200	2,000	1,500
Boulder, Colorado	2/11 - 2/25, 2009	Thornton et. el,.2010	450	300	200
Calgary, Alberta	4/16 - 4/21, 2010	Mielke et al., 2011	250	500	300
Los Angeles, California	5/15 – 6/15, 2010	Mielke et al., 2010	2,550	2,700	4,000

Figures

Figure 1. Predicted mean fine particulate chloride without the heterogeneous $ClNO_2$ production in (a) February and (b) September. Predicted mean coarse particulate chloride without the heterogeneous $ClNO_2$ production in (c) February and (d) September. A comparison of predicted fine particulate chloride with observed data from the Interagency Monitoring of PROtected Visual Environments (IMPROVE) network in (e) February and (f) September.

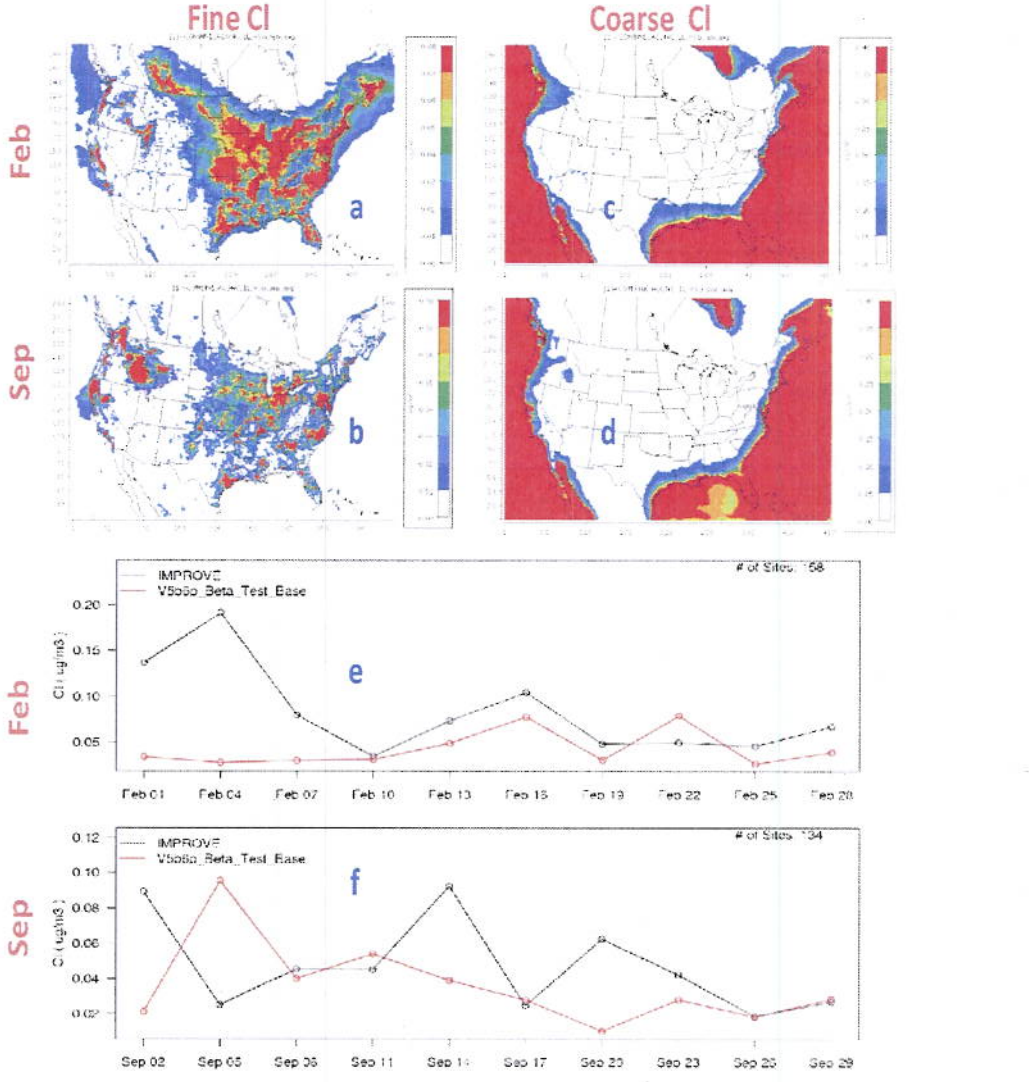

Figure 2. (a) Predicted mean yield for $ClNO_2$ on fine particles in (a) February and (b) September. Predicted mean yield for $ClNO_2$ on coarse particles in (c) February and (d) September.

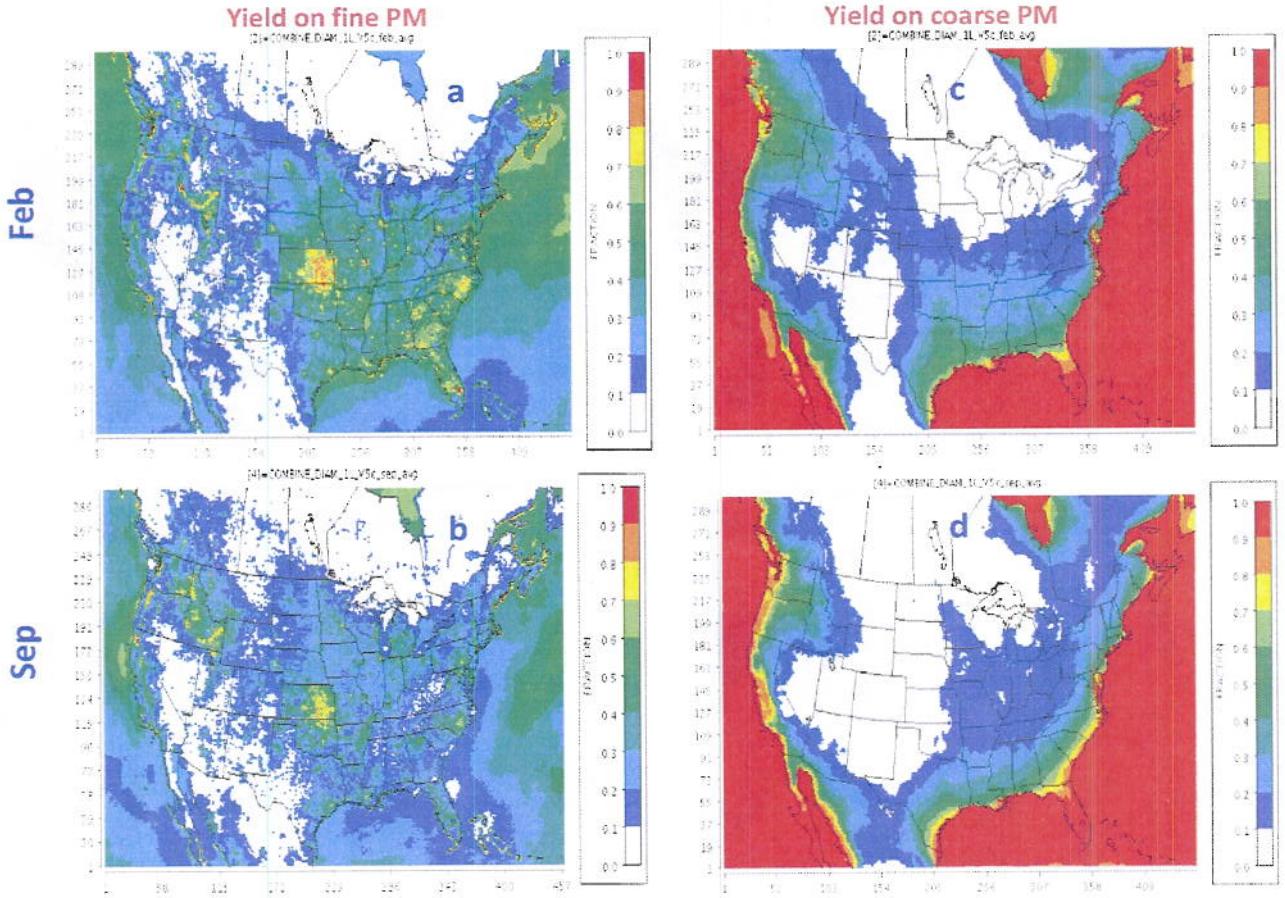

Figure 3. Predicted mean $ClNO_2$ in (a) February (b) September and maximum $ClNO_2$ in (c) February (d) September. It should be noted that the largest hourly value for each grid-cell in the entire month is shown in (c) and (d).

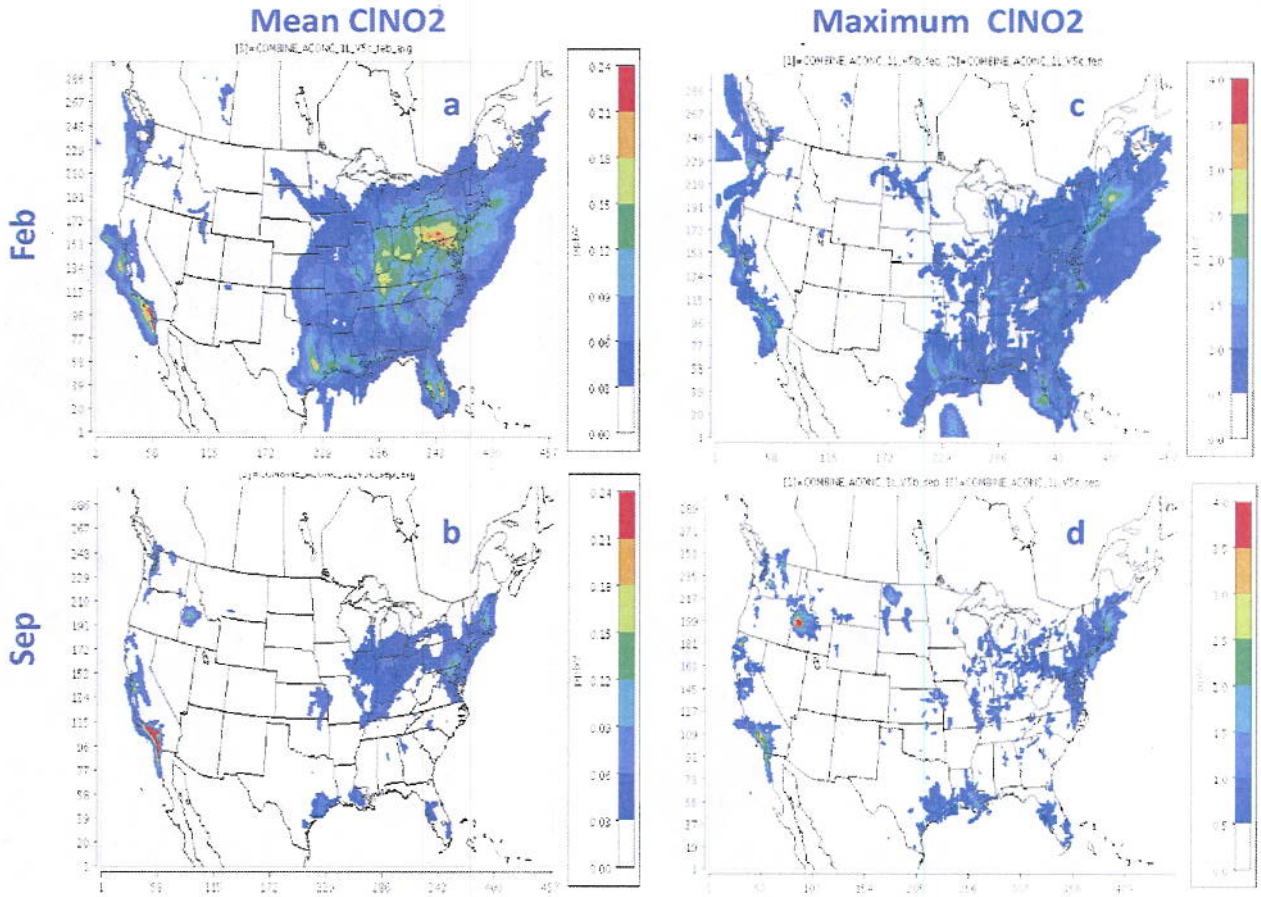

Figure 4: Impact of the heterogeneous $ClNO_2$ production on O_3: (a) mean O_3 without the heterogeneous production in February (b) mean O_3 without the heterogeneous production in September (c) increases in mean O_3 due to the heterogeneous production in February (d) increases in mean O_3 due to the heterogeneous production in September.

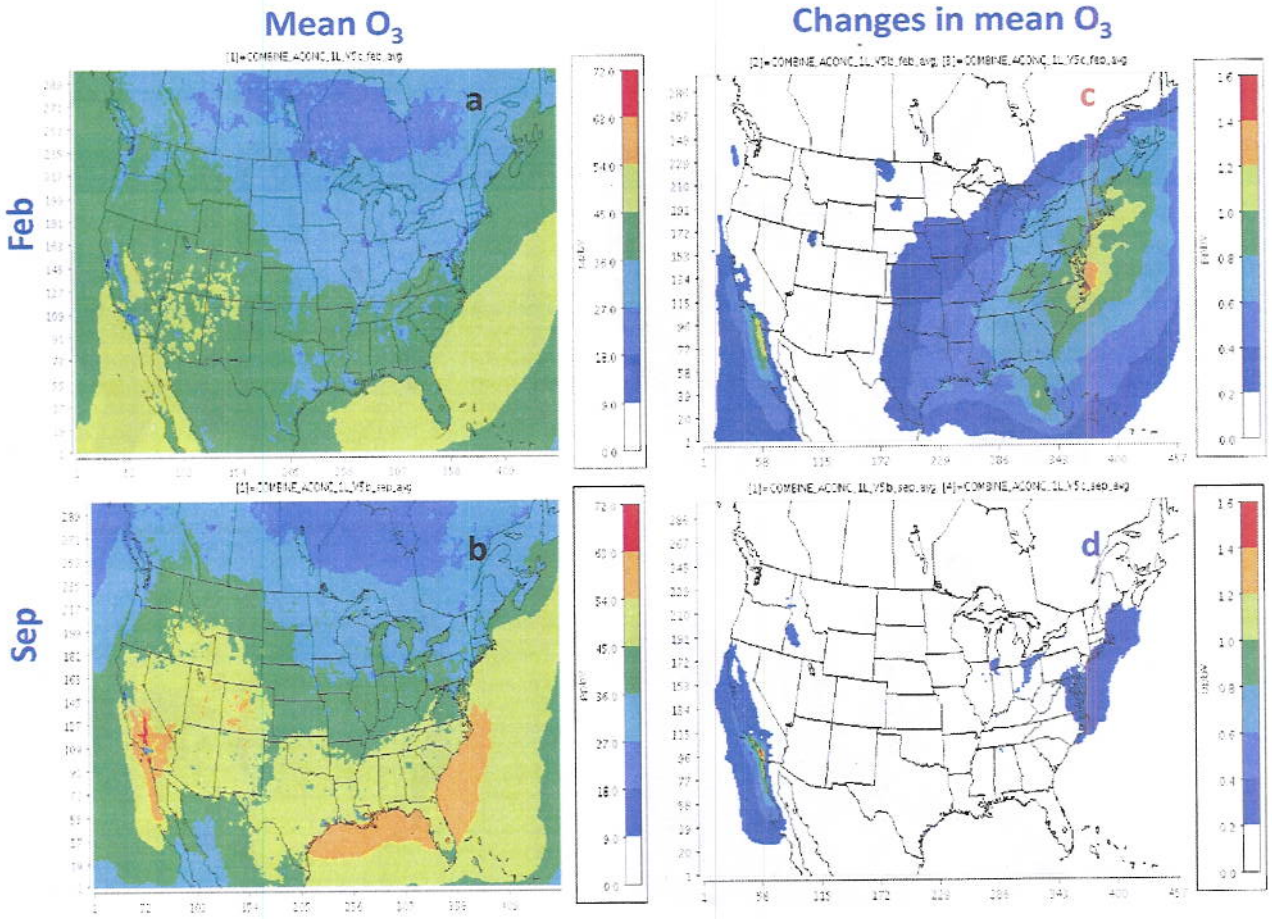

Figure 5: Impact of the heterogeneous $ClNO_2$ production on TNO_3 (HNO_3 + aerosol nitrate): (a) mean TNO_3 without the heterogeneous production in February (b) mean TNO_3 without the heterogeneous production in September (c) decreases in mean TNO_3 due to the heterogeneous production in February (d) decreases in mean TNO_3 due to the heterogeneous production in September

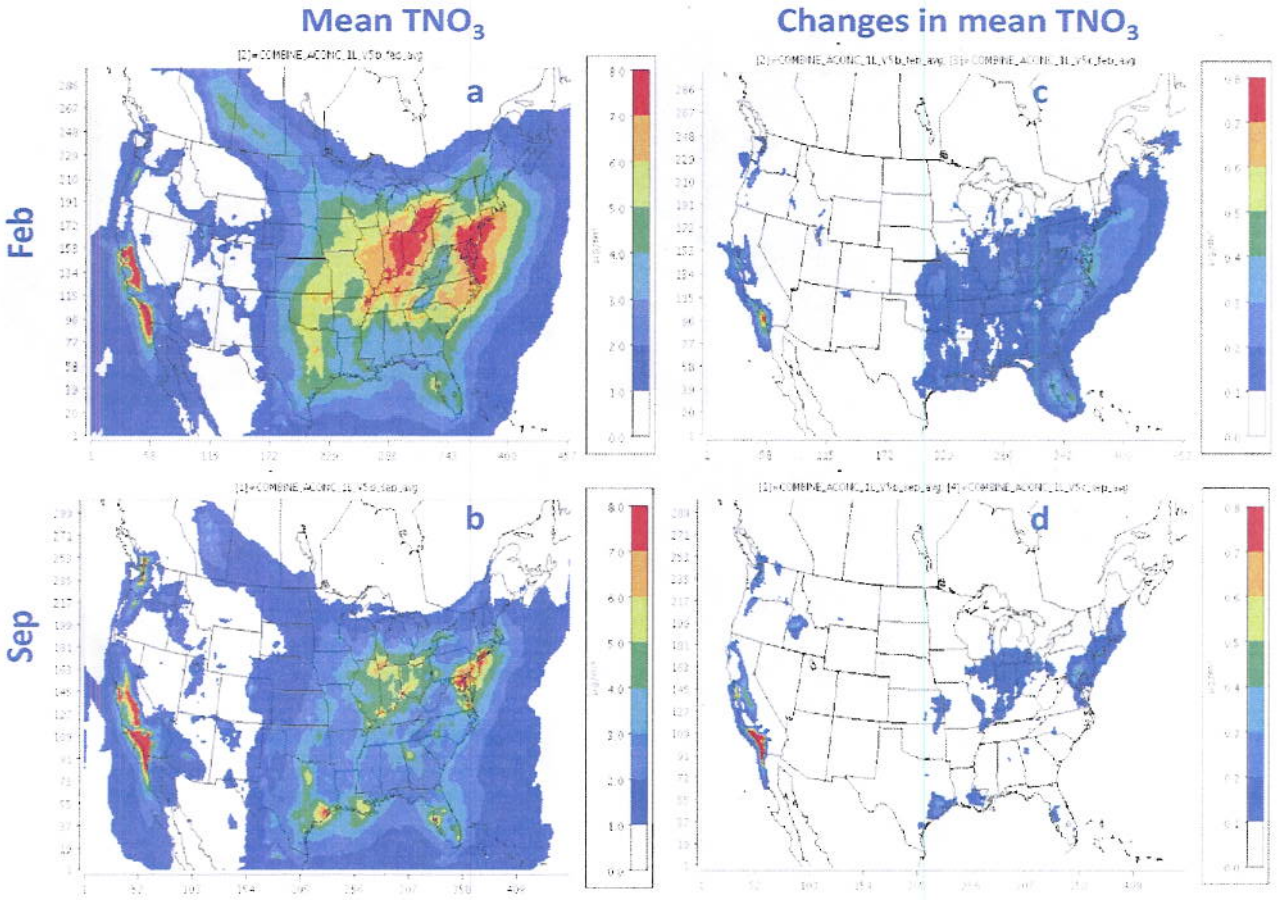

Figure 6: Time series of the absolute value of changes in $ClNO_2$, O_3, and $-TNO_3$ at (a) Los Angeles in February (b) Los Angeles in September (c) Indiana in February (d) Idaho in September. All Δ values are positive for O_3 and $ClNO_2$ and negative for TNO_3.

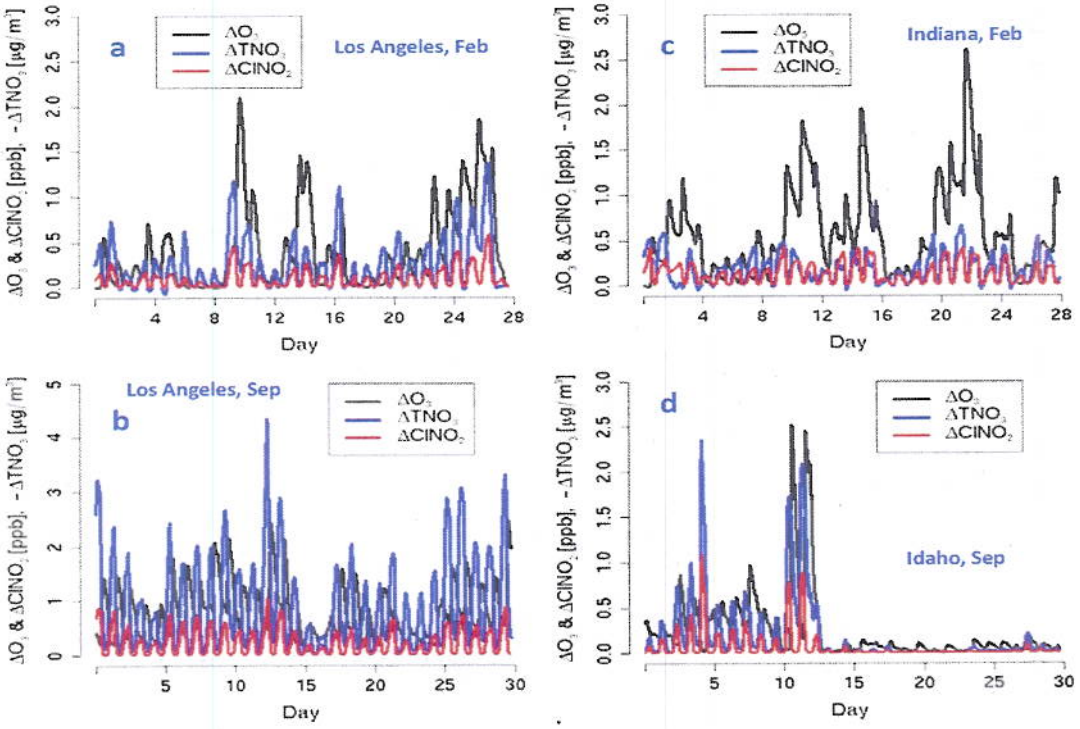

Figure 7: Diurnal absolute value of changes in $ClNO_2$, O_3, and $-TNO_3$ at (a) Los Angeles in February (b) Los Angeles in September (c) Indiana in February (d) Northeastern United States in September. All Δ values are positive for O_3 and $ClNO_2$ and negative for TNO_3.

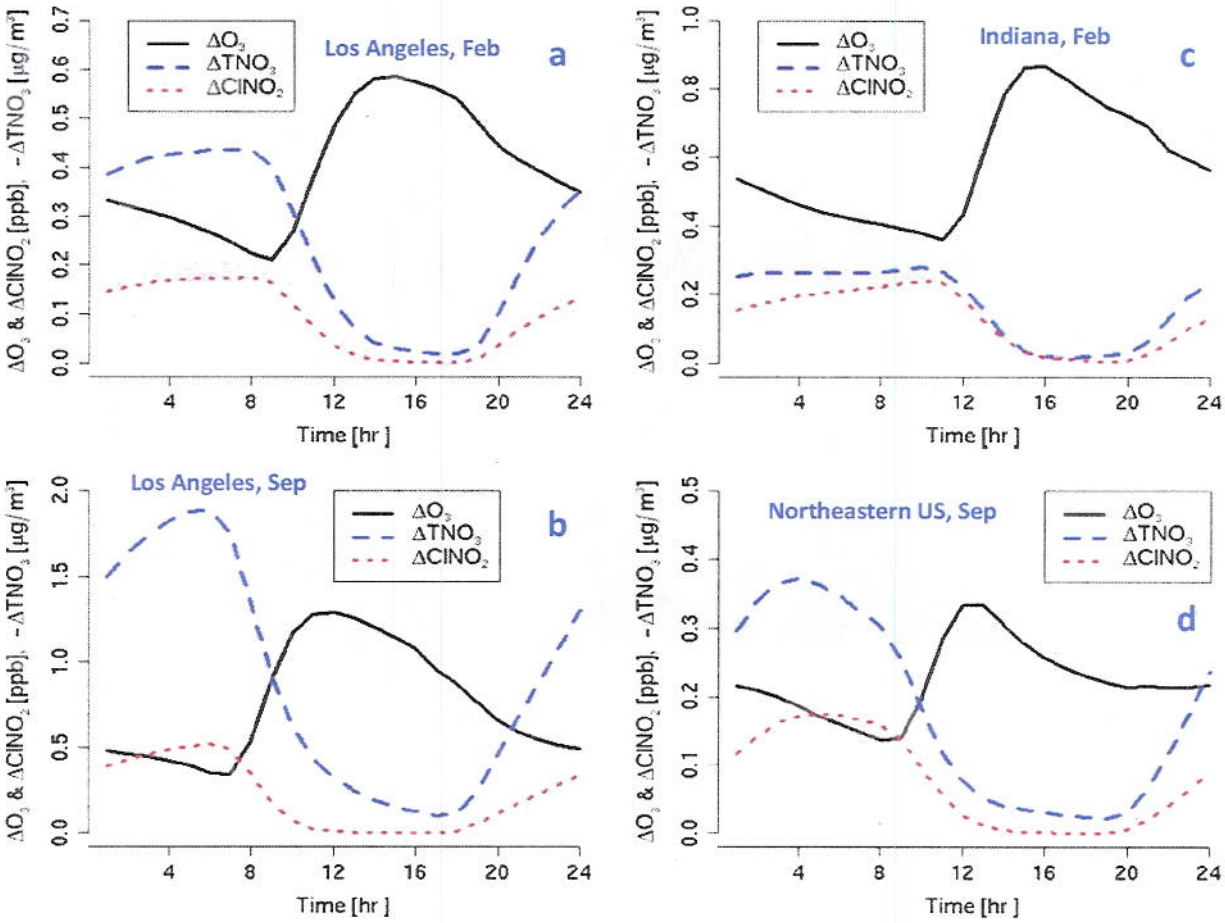

Figure 8: (a) Predicted mean 8-hr O_3 in February (b) Predicted mean 8-hr O_3 in September (c) changes in mean 8-hr O_3 due to the heterogeneous production in February (d) changes in mean 8-hr O_3 due to the heterogeneous production in September.